Eur. Phys. J. B **1**, 319–326 (1998)

THE EUROPEAN PHYSICAL JOURNAL B

Existence, stability and structure of a hexagonal phase doped with nanoparticles

L. Ramos[1,a], P. Fabre[2], and R. Ober[1]

[1] Laboratoire de Physique de la Matière Condensée, Collège de France[b], 11 Place Marcelin Berthelot, 75231 Paris Cedex 05, France
[2] UMR CNRS-Elf Atochem, 95 rue Danton, 92303 Levallois-Perret Cedex, France

Received: 4 September 1997 / Revised: 14 October 1997 / Accepted: 19 November 1997

Abstract. We describe and study by small-angle X-ray scattering (SAXS) a new type of hybrid system. It is composed of a swollen lyotropic hexagonal phase into the cylinders of which solid magnetic particles of nanometric size have been incorporated. It has been found to be stable for volume fractions of particles up to 2% provided the cylinders are sufficiently large. A unidimensionnal magnetic liquid is thus realized. The structural properties of this colloidal assembly have been investigated by SAXS, and the specific features of the scattering spectra are analysed and interpreted. One of the remarkable results is the evidence of depletion interactions between the particles and the inner walls of the cylinders inside which particles are located.

PACS. 75.50.Mm Magnetic liquids – 82.70.Dd Colloids – 61.10.-i X-ray diffraction and scattering

1 Introduction

Hybrid systems, composed of solid particles included into lyotropic organized liquid phases have recently gained interest [1–4], and are currently a subject of several studies. Their interest arises from the fact that they combine two elements of different nature, and display not only the properties of each of their constituents, but additional properties due to the coupling between them. In particular, recent studies have shown that under well-defined conditions [5,6], it was possible to trap solid particles between the fluctuating planes of a swollen lamellar phase, and that the resulting doped system displays very original magnetic and elastic properties [7,8]. In the same line of thought, one may infer that a colloidal assembly of particles unidimensionally confined inside a hexagonal matrix should exhibit new and interesting behaviors. However, the confinement of colloidal objects in a surfactant structure requires one to fulfill some conditions among which the most obvious is a matching between the characteristic sizes of the two constituting objects. In a first step we have shown that it is possible to considerably swell the surfactant matrix of a lyotropic hexagonal phase [9]. It thus allows in a second step the realization of doped hexagonal systems, which is described here.

This new type of hybrid system, which combines the two-dimensional long- range order of an hexagonal phase with the gas-like disorder of a suspension of particles, allows one to address original questions concerning its structure, such as for instance the effect of solid particles on the true long-range positional order of the columns, or reversibly the anisotropy of the spatial arrangement of the grains confined inside the cylinders. Finally, the existence of a doped swollen hexagonal phase, and the knowledge of its structure, could lay the foundation for the synthesis and use of new materials, such as mesoporous membranes [10].

The remainder of the paper is the following. In the first part, we investigate the existence and stability of a doped hexagonal phase and choose for that purpose magnetic particles because of their ability to orient under a magnetic field. In the second part the specific features of the small-angle X-ray scattering spectra of the phases are presented and discussed. The interpretation given in the third part allows the spatial distribution of the particles with respect to the cylinders to be determined.

2 Existence and stability of doped hexagonal phases

2.1 The two constituents

The first constituent of the hybrid system is a ferrofluid prepared with the method described in references [11,12].

[a] *Present address*: Department of Physics, University of Pennsylvania, 2095, 33rd Street, Philadelphia, PA 19104-6396, USA. e-mail: `laurence@dept.physics.upenn.edu`
[b] CNRS, URA 792

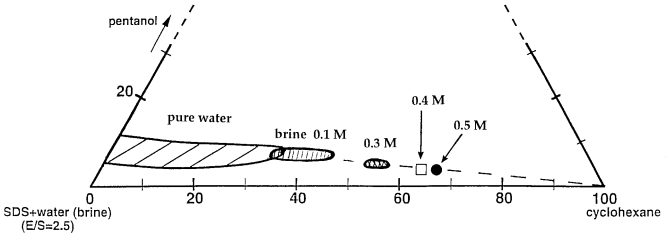

Fig. 1. Superposition of the phase-diagrams (weight percent) of the pseudo-ternary systems sds+water (brine)/pentanol/cyclohexane. The phase-diagrams are made for various polar solvents, namely pure water and brine 0.1 M, 0.3 M, 0.4 M and 0.5 M. The weight ratio water (brine)/sds is set at 2.5. The regions of stability for the non doped hexagonal phases are dashed. Notice that for high salt concentrations (0.4 and 0.5 M), these regions are so narrow that they are represented by points (square and circle) on the graph. The dashed curve is a guide for the eye showing that the extrapolation of the hexagonal zones lies in the cyclohexane corner. Only the phases with sufficiently large cylinders (brine 0.4 and 0.5 M) can be doped.

It consists of maghemite ($\gamma-Fe_2O_3$) particles stabilized in cyclohexane by adsorbed organophosphorated surfactant molecules. This colloidal suspension is superparamagnetic due to the small sizes of the grains which are magnetic monodomains. The size distribution of the grains follows a log-normal law, with a iron oxide core radius $r_0 = 35$ Å ($\ln r_0$ is the mean value of $\ln r$) and standard deviation $\sigma = 0.35$, as determined by SAXS (see below). The ferrofluid samples are defined by their volume fraction in particles Φ.

The second constituent is a quaternary mixture of water, cyclohexane, sodium dodecyl sulfate (sds) as surfactant and pentanol as cosurfactant. This lyotropic system displays at room temperature a direct hexagonal phase [13], constituted of infinite nonpolar cylinders, arranged in an hexagonal array in water, and whose radius R ranges between 15 and 54 Å. It has been previously shown [9] that the increase of the ionic strength of the continuous medium allowed the increase of the range of stability for the radius of the cylinders: by replacing water with brine of ionic force ranging from 0.1 to 0.5 M, it is possible to monitor the radius of the non polar cylinders over one decade, up to 168 Å, while keeping the distance between adjacent cylinders small and nearly constant (about 25 Å). The location of the hexagonal zones for different salt concentrations are displayed in cross-sections of a pseudo-ternary phase diagram (Fig. 1).

2.2 The doped systems

The hybrid systems are obtained by replacing cyclohexane with ferrofluid in the quaternary mixture. When the cylinders of the initial system are not dilated enough, it is not possible to obtain a stable phase and the doping process leads to unstable systems characterized by the coexistence of aggregates of solid particles and a lyotropic mesophase. On the contrary, stable doped phases are obtained for sufficiently swollen systems. The phases can incorporate particles up to a volume fraction Φ of 2%, with a swelling ratio, defined by the volume fraction of oil, varying between 0.67 and 0.70. The upper value of this range of stability is limited by the maximum swelling ratio of the hexagonal matrix, 0.70 (see the phase-diagrams Fig. 1 for the location of the doped systems). It is important to note that the occurrence of a doped hexagonal phase had already been observed [13] as a component of a polyphasic system, but that attempts to isolate and characterize it had been unsuccessful.

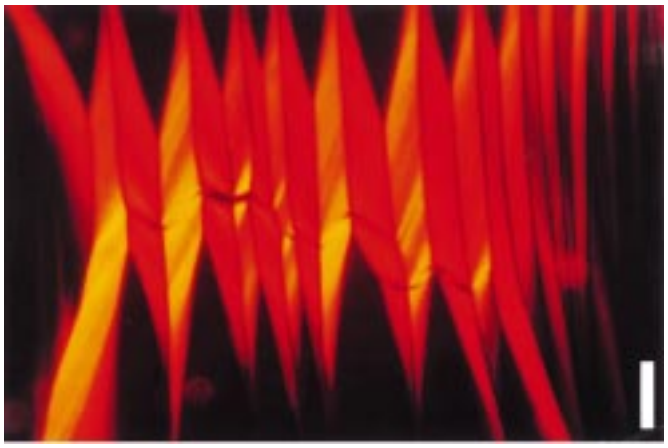

Fig. 2. Typical texture of a swollen and doped ($\Phi = 0.25\%$) lyotropic hexagonal phase. bar = 100 μm.

Macroscopically, the doped samples appear very similar by their viscosity and transparency to their non-doped homologous systems, except for a deep color due to the iron oxide particles. The microscopic observation of the samples held in glass capillaries with a rectangular cross-section (100 μm × 1 mm) allows one to identify the stable doped hexagonal phases: between crossed polarizers a texture commonly referred to as fan-shaped [14] appears, uniformly colored as the initial ferrofluid (see Fig. 2). A sketch of the doped systems, that schematically shows the location of the magnetic grains inside the apolar cylinders of the direct hexagonal phases, is given in Figure 3.

The geometric parameters of the host matrix have been previously determined [9]. For the less swollen stable doped systems (ferrofluid volume fraction 0.67), the corresponding non doped system has a lattice parameter d_c equal to 325 Å, with apolar cylinders of radius R equal to 150 Å, and thus a distance between adjacent cylinders ($d_c - 2R$) equal to 25 Å. It is interesting to emphasize that, for particles of diameter about 100 Å (including the surfactant layer, of thickness 16 Å [15]), the minimum diameter required for the cylinders is 300 Å. This is substantially different from the case of lyotropic lamellar phases, where the same particles could be included in very narrow oil layers of 110 Å: a unidimensional confinement seems thus much more demanding in terms of steric hindrance than a bidimensional one.

To summarize, we have shown that it was possible to trap colloidal magnetic particles inside the nonpolar

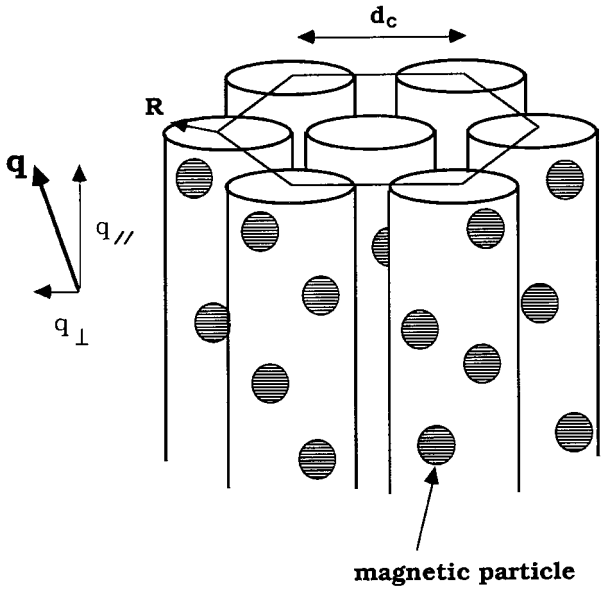

Fig. 3. Schematic representation of the lyotropic hexagonal phase doped with magnetic particles suspended in oil. Projection of the wave-vector into perpendicular and parallel components with respect to the long axis of the cylinders.

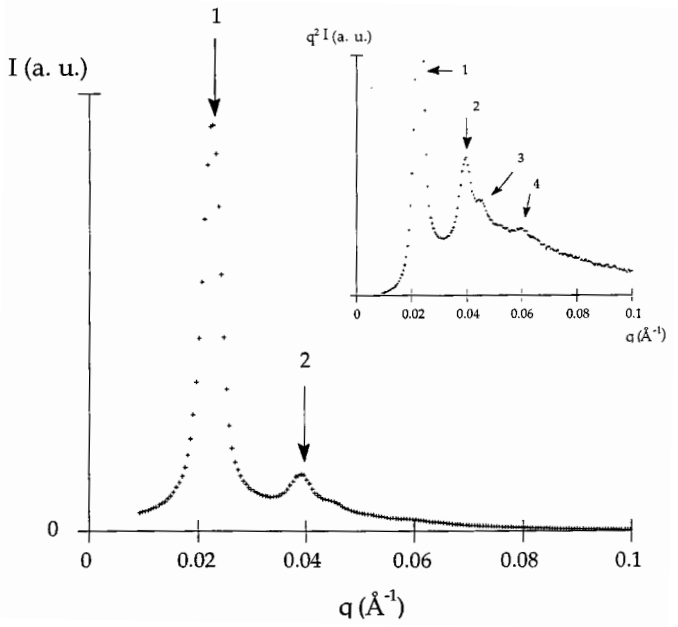

Fig. 4. *I versus q* spectrum of the non-doped hexagonal phases in arbitrary unit. The arrows indicate the location of the Bragg peaks. The q^2I *versus* q plot (inset) enables one to better visualize the third and fourth orders. The positions of the peaks are the following: 0.0223; 0.0392; 0.0449; 0.0591 Å^{-1}.

cylinders of a swollen lyotropic hexagonal phase up to a volume fraction of 2%, provided the cylinders are large enough (diameter more than twice the diameter of the particles). Besides the magnetic properties, the existence of such a system appears by itself very interesting because it *a priori* combines the long-range order of a bidimensional lattice of cylinders and the gas-like disorder of the colloidal particles. These apparently opposite features have incited us to closely study by small-angle X-ray scattering (SAXS) the structural properties of the systems.

3 X-ray scattering results

3.1 Sample and experimental set-up

Since the stability range for the doped samples in terms of swelling ratio is very narrow, we focus on one swollen system (weight ratios: brine [0.4M]/sds = 2.5; oil/sds = 6.46) and essentially explore Φ, the particles volume fraction (relative to cyclohexane), as relevant parameter, that we vary between 0.15 to 2%. We note Φ_0, the particles volume fraction relative to total volume, which here stands in the range 0.1-1.3%. We also studied for comparison, on one hand hexagonal samples without particles, and on the other hand isotropic ferrofluids of the same particles. The samples are held in sealed Lindeman capillaries of 1 mm diameter; the doped hexagonal samples are oriented with the lyotropic cylinders parallel to the long axis (z) of the capillary, with the following process: the hexagonal is first cooled down to an isotropic state ($\sim$ 8 °C) and then slowly heated up to room temperature under an homogeneous and constant magnetic field ($H \sim 10$ kG), along which the cylinders align [16]. Concerning the experimental X-ray set-up, the distance between the sample and the linear counter was fixed at 0.8 m, the scattering wavevectors ranging between 9×10^{-3} and 0.17 Å^{-1} and the instrumental width being approximately 3×10^{-3} Å^{-1}. We have positioned the sample-holder in two perpendicular directions within the diffusion plane, so as to set the wave-vector **q** either normal ($q_\perp$) or parallel ($q_{//}$) to the long-axis of the cylinders.

3.2 The two constituents

3.2.1 The non-doped hexagonal phase

The spectrum of the non-doped system is given in Figure 4. Its features described below are commonly encountered with hexagonal liquid crystal systems [17,18]: it displays four Bragg peaks, whose positions are in the ratio 1, $\sqrt{3}$, 2 and $\sqrt{7}$, and a negligible scattering when the wavevector q tends to 0. Compared to usual lyotropic hexagonal phases, the main difference here is that the locations of the peaks are shifted to smaller q because of the considerable swelling ratio of this phase. From the position q_0 of the first order Bragg peak, the lattice parameter of the triangular array is derived: $d_c = \frac{2}{\sqrt{3}} \frac{2\pi}{q_0} = 325$ Å, and from the composition of the lyotropic mixture, the radius R of the non-polar cylinders can be calculated [9]: $R = 150$ Å. The full-width of the first order peak at half-maximum intensity is 4×10^{-3} Å^{-1} and corresponds approximatively to the instrumental width.

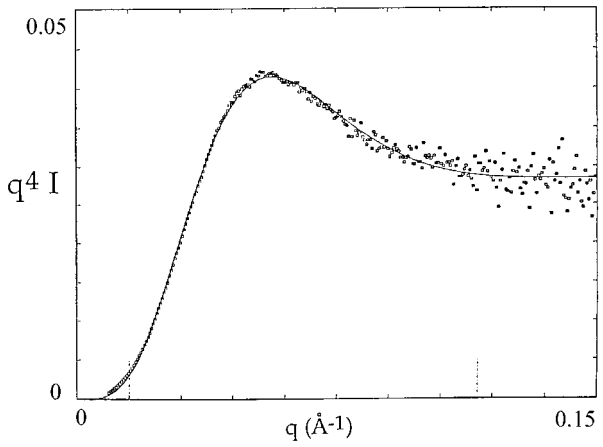

Fig. 5. Fit on a q^4I *versus* q plot for an isotropic ferrofluid sample ($\Phi = 0.25\%$) allowing the determination of the size distribution of the colloids ($r_0 = 35$ Å, $\sigma = 0.35$).

3.2.2 The isotropic ferrofluid samples

The signal of a dilute isotropic ferrofluid sample enables one to characterize the size distribution of the colloidal particles. Indeed, the scattered intensity of N non-interacting particles is given by:

$$I(q) \propto N \int_0^\infty \mathcal{D}(r) P(q,r) \mathrm{d}r \qquad (1)$$

where $\mathcal{D}(r) = \frac{1}{\sqrt{2\pi}\sigma r} \exp\left[-\frac{1}{2\sigma^2}\left(\mathrm{Ln}\frac{r_0}{r}\right)^2\right]$ is the log-normal distribution function of the suspension and

$$P(q) = \Delta\rho^2 \left[\frac{\sin(qr) - qr\cos(qr)}{q^3}\right]^2$$

is the form factor of a sphere of radius r with $\Delta\rho$ as contrast [19]. In view of the relative electronic densities for the different species (cyclohexane $\rho(\mathrm{cyclo}) = 0.267\mathrm{e}^-\text{Å}^{-3}$, tails of the surfactants coating the particles $\rho(\mathrm{tail}) = 0.275\mathrm{e}^-\text{Å}^{-3}$, core of the magnetic particles $\rho(\mathrm{Fe_2O_3}) = 1.452\mathrm{e}^-\text{Å}^{-3}$), only the iron oxide core of the particles is seen here. A fit of the experimental data with (1), performed on a Porod plot (q^4I *versus* q) enables the determination of the parameters of the size distribution function: one obtains a mean radius $r_0 = 35$ Å and a standard deviation $\sigma = 0.35$ (Fig. 5).

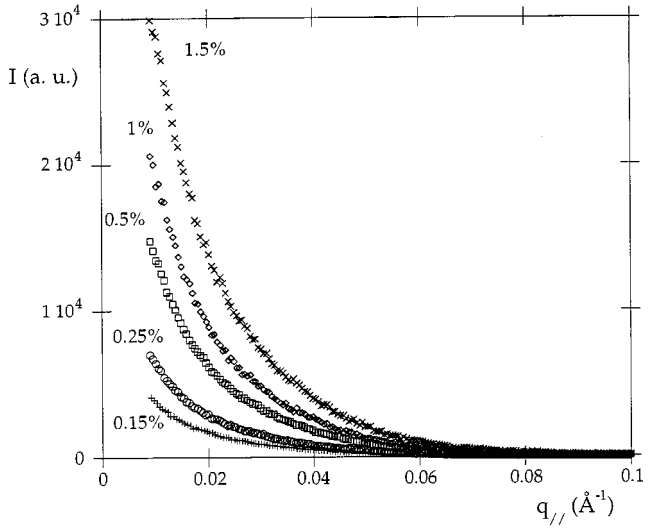

(a)

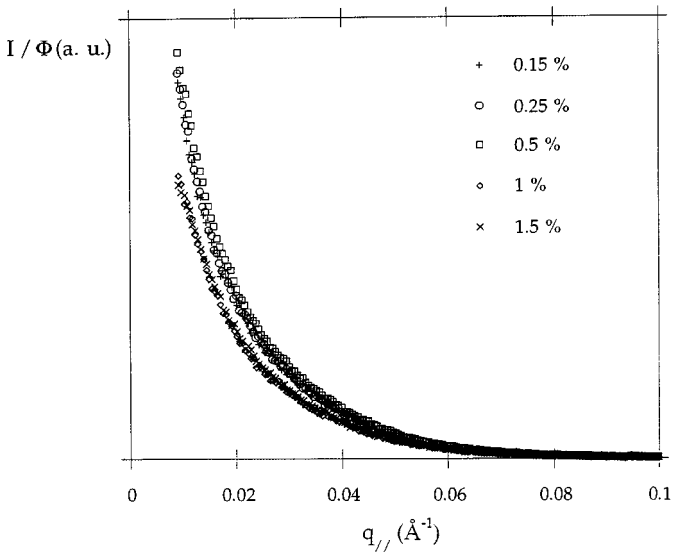

(b)

Fig. 6. $q_{//}$-spectra of hexagonal phases with various Φ (0.15%; 0.25%; 0.5%; 1%; 1.5%). (a) I *versus* q plot. (b) I/Φ *versus* q plot.

3.3 The doped hexagonal samples

3.3.1 Hexagonal structure

The $q_{//}$-spectra and $q_\perp$-spectra are respectively given in Figures 6 and 7, in I (a) and I/Φ (b) *versus* q plots, for Φ in the range 0.15-1.5%. The $q_{//}$- and $q_\perp$-spectra clearly exhibit different features. Both display a strong central diffusion (central diffusion is defined as the intensity scattered for wavevectors smaller than the first order Bragg peak). Additionally, the $q_\perp$-spectra display peaks, whose positions in the ratio 1, $\sqrt{3}$, 2, $\sqrt{7}$, are the signature of an hexagonal order. The location of the peaks permits the determination of the lattice parameter of the doped hexagonal phases: the values do not show any variation with the volume fraction in particles (Fig. 8). Moreover, regardless of the particle concentration, the full-width at half-maximum intensity remains 4×10^{-3} Å^{-1} (*i.e.* of the same order of magnitude as for the non-doped system). These two observations indicate that the solid particles

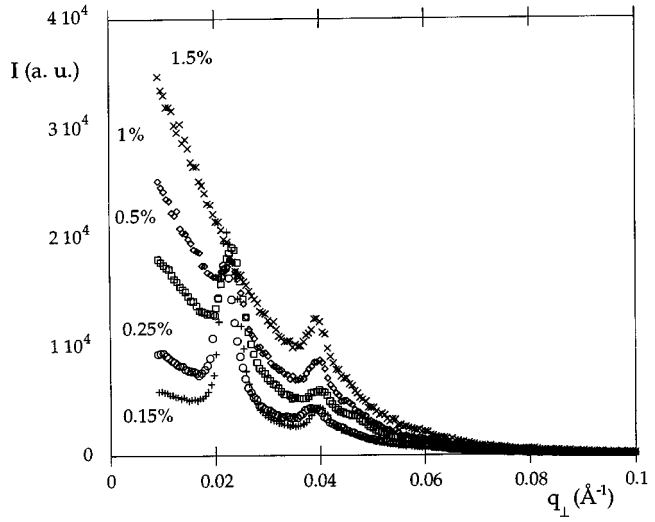

(a)

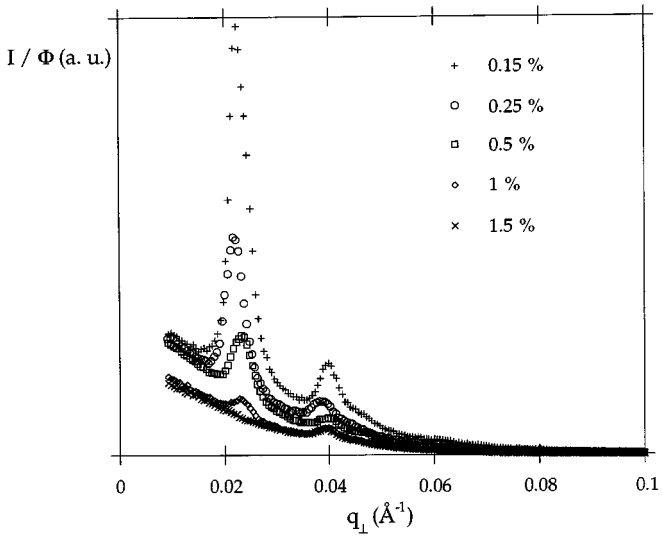

(b)

Fig. 7. $q_\perp$-spectra of the same samples as in Figure 6; the symbols and units are also the same as in Figure 6. (a) *I versus q* plot. (b) I/Φ *versus q* plot.

do not seem to disturb the long-range positional order of the lyotropic cylinders. However, the heights of the peaks, and especially the first order diffraction one, are strongly affected by the variation of concentration. In particular, the first order is not detectable for $\Phi = 1.5\%$, while the second order peak remains clearly observable. For higher Φ (1.7 and 2%) the first order peak is recovered (see the inset of Fig. 11). This point will be interpreted in the following section.

As for the $q_{//}$-configuration, the systematic absence of peaks for the spectra confirms that there are no hexagonal domains with their optical axis perpendicular to the z axis of the capillary. Moreover, the systematic presence of Bragg peaks at fixed positions for the $q_\perp$-spectra reveals a cylindrical symmetry of the hexagonal domains with respect to the z axis. One can evaluate more precisely the mosaicity of the sample, by investigating the scattering patterns when the direction of **q** continuously varies from perpendicular to parallel to z. In that way, we have estimated that samples have a mosaicity less than 10 deg. They can therefore be reasonably considered as bidimensional powders.

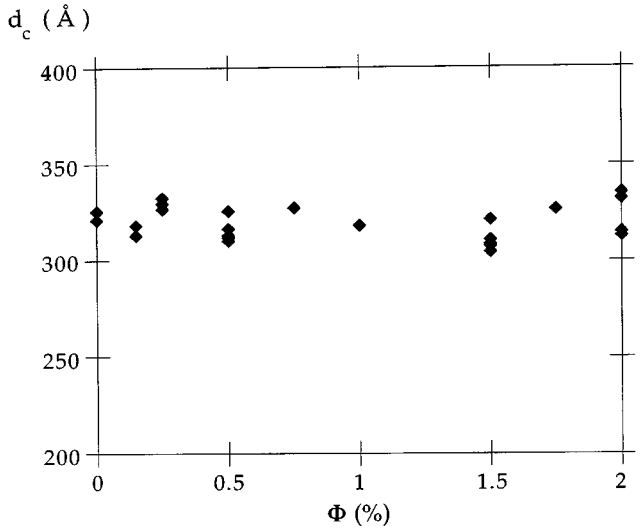

Fig. 8. Lattice parameters of the doped hexagonal phases *versus* Φ as determined from the $q_\perp$-spectra.

3.3.2 Size distribution of the confined particles

For low Φ, Figures 6b and 7b show that the central diffusions superimpose for the $q_{//}$- and $q_\perp$-spectra in a I/Φ representation. For the more concentrated systems ($\Phi = 1$ and 1.5%), one can notice a slight decrease of the small-angle scattering. To compare the central diffusion of the $q_{//}$- and $q_\perp$-spectra, we have plotted (Fig. 9) $I(0)/\Phi$ *versus* Φ, where $I(0)$ is obtained from extrapolation to the origin of Guinier plots ($\ln(I)$ *versus* q^2). The values are of the same order of magnitude. At a first order of approximation the central diffusion for the doped hexagonal samples is thus isotropic and proportional to the volume fraction of particles.

The $q_{//}$-signals can be directly compared to the signal of isotropic ferrofluid. The intensities, once normalized with respect to Φ_0, the volume fraction of particles relative to the total volume, perfectly superimpose with the normalized intensity scattered by an isotropic ferrofluid sample, as displayed in Figure 10a, in a Porod plot. We should emphasize here that this is obtained without any adjusting parameter, concerning the intensity for instance. This feature along with the consistency of the asymptotic behaviour (Fig. 10b) strongly supports the fact that the colloids once confined inside the cylinders do not suffer

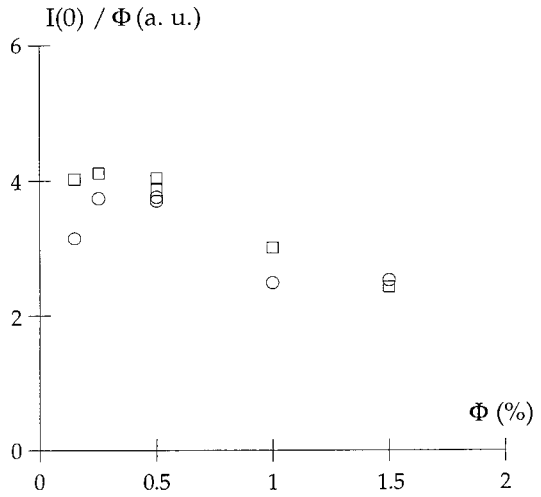

Fig. 9. $I(0)/\Phi$ *versus* Φ plots for hexagonal samples; $I(0)$ is obtained from extrapolation to the origin of Guinier plots ($\ln I$ *vs.* q^2); ($\square$)$q_\perp$-spectra, ($\bigcirc$)$q_{//}$-spectra.

any reorganization or aggregation in the range of concentration explored. This assertion is reinforced by an analysis in terms of size distribution for the colloids of the different spectra, which gives comparable characteristics to those of an isotropic ferrofluid sample ($r_0 = 34$ Å and $\sigma = 0.36$). This yields a relevant result, which is that the particles do not aggregate in the cylinders.

Recalling that we observe a central diffusion, at first order isotropic, and in particular equal for the $q_{//}$ and $q_\perp$ orientations, the above comparison with an isotropic ferrofluid sample reveals then that the spatial distribution of the particles is pseudo-isotropic. This is due to the fact that the samples are 2D-powder: when **q** is perpendicular to the cylinders, the scattered intensity is therefore averaged over the different crystallites and at small q, one recovers a gas-like spatial distribution of the particles.

4 Spatial distribution of the particles in the cylinders

As previously indicated, the intensities of the Bragg peaks strongly vary with Φ, the volume fraction of particles. To illustrate that point, we have plotted in Figure 11 the ratio A_1/A_2, where A_1 (resp. A_2) is the integrated intensity of the first (resp. second) order diffraction peak, *versus* Φ; this ratio displays a non monotonous variation. Notice that there is no experimental data for Φ equal 0: without particles, one cannot control the orientation of the samples, which makes a direct comparison of the data with and without particles irrelevant. It is well-known that the form factor of the scattering objects can be responsible for strong variation of the intensities of the diffraction peaks. On general grounds, the form factor of coaxial cylinders

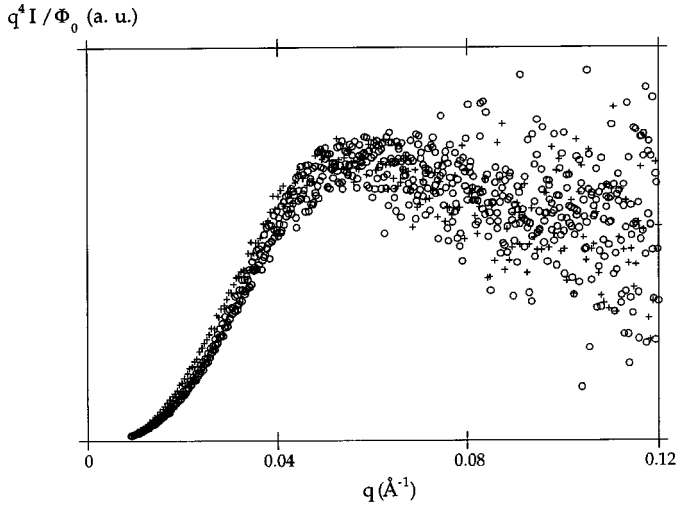

(a)

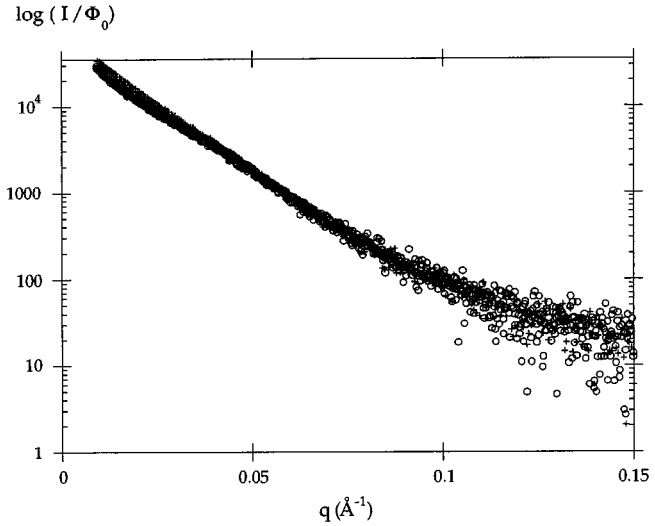

(b)

Fig. 10. (a) $q^4 I/\Phi_0$, (b) $\log I/\Phi_0$, *versus* q plots. The points are the $q_{//}$-spectra of doped hexagonal samples (same as in Fig. 6, with Φ_0 equal to 0.10; 0.17 and 0.34%) and the black dots are from an isotropic ferrofluid sample ($\Phi_0 = 0.17\%$).

of infinite length is expressed as $P(q) = |F(q)|^2$ with [20]:

$$F(q) = \frac{2}{q} \frac{\sum_{j=1}^{n} (\rho_j - \rho_{j+1}) R_j J_1(qR_j)}{\sum_{j=1}^{n} (\rho_j - \rho_{j+1}) R_j^2} \cdot \qquad (2)$$

Here, ρ_j and R_j ($1 \leq j \leq n$) stand respectively for the density and radius of the jth cylinders, ρ_{j+1} is the density of solvent surrounding the cylinders ($0.337 e^- Å^{-3}$) and J_1 the first Bessel function.

For the non-doped system, we consider two coaxial cylinders (Fig. 12), a cylinder of cyclohexane ($R_1 = 150$ Å,

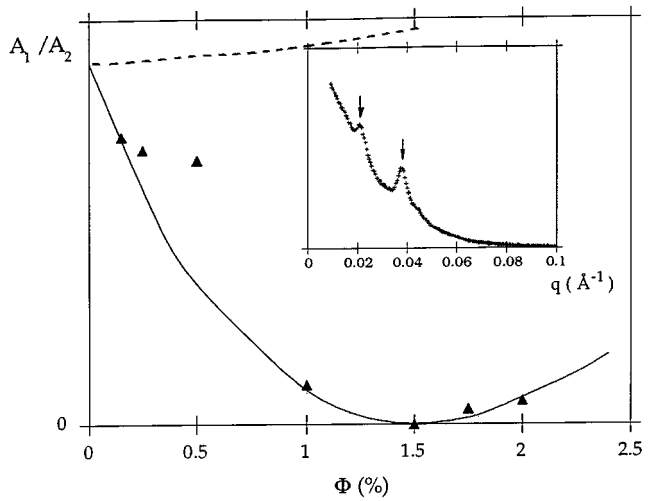

Fig. 11. Symbols: plots of the integrated intensity of the first order (A_1) over the second order (A_2) peak *versus* Φ; full line: theoretical curve calculated as explained in the text in the case of a depletion; dashed line: theoretical curve in the case of a uniform distribution. Inset: $q_\perp$-spectra of a doped hexagonal samples ($\Phi = 2\%$), showing that the first order is recovered for Φ higher than 1.5%.

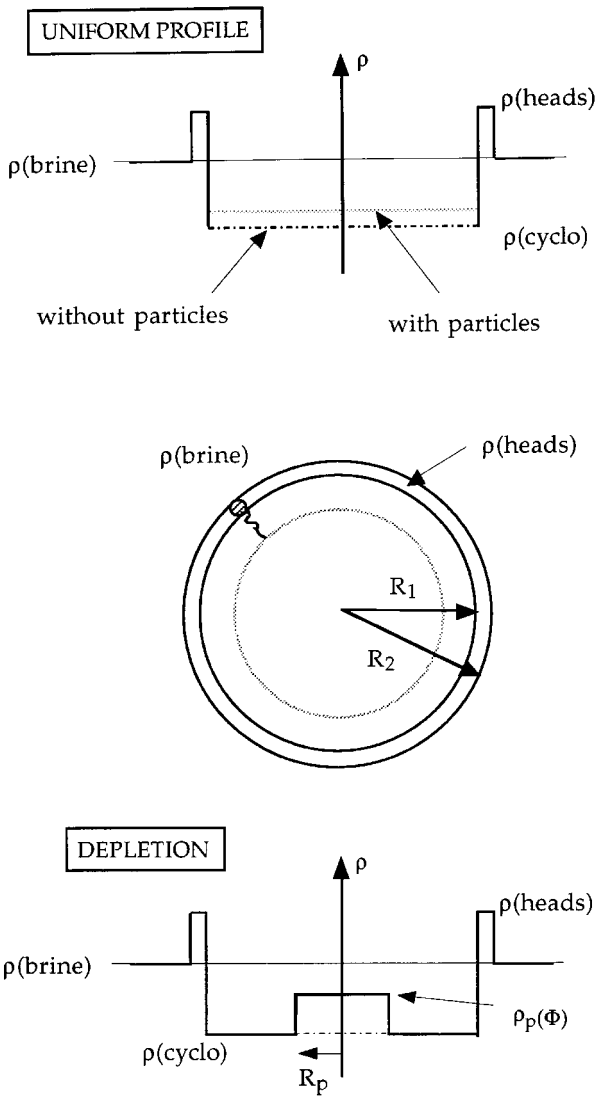

Fig. 12. Density profiles for the doped cylinders; top: uniform profile for the apolar core; bottom: non-uniform profile for the apolar core, in the case of a depletion.

$\rho(\text{cyclo}) = 0.267\text{e}^{-}\text{Å}^{-3}$), and a shell for the surfactant heads (thickness 6 Å, $\rho = 0.395\text{e}^{-}\text{Å}^{-3}, R_2 = 156$ Å). Notice that for the sake of simplicity, the corona of the sds tails is included in the inner cylinder. The smallest q for which the form factor of the non-doped cylinder equals zero is then equal to 0.0265 $\text{Å}^{-1}$and is thus rather close to the position of the first-order Bragg peak (0.0223 Å^{-1}) for the hexagonal lattice.

For the doped phase, one has to consider the modification of the form factor induced by the particles. In a first approximation, one can consider a uniform distribution of the particles inside the inner core of radius R_1 and one thus averages the ferrofluid electronic density as the weighted densities of particles and solvent: $\bar{\rho} = \Phi\rho(\text{Fe}_2\text{O}_3) + (1-\Phi)\rho(\text{cyclo})$. Owing to the very weak range of averaged ferrofluid density (0.269-0.291$\text{e}^{-}\text{Å}^{-3}$ for Φ ranging between 0 and 2%), no significant variation of the $P(q)$ curves with Φ is depicted. One therefore has to assume a non uniform density for the particles, with a tendency for the particles either for depletion or for adsorption. We choose a step profile, which is simple but yet very realistic since it naturally introduces a characteristic length for the particle/cylinder interactions. The form factor is then computed with a set of three coaxial cylinders. A higher density at the periphery of the non polar cylinder, which would account for a trend towards adsorption, leads to an increase of q^*, the smallest q for which the form factor $P(q)$ equals zero, with Φ, and is therefore inconsistent with experimental results. On the contrary, a higher density in the centre is in agreement with experiments, since q^* is found to decrease with Φ. We note R_p, the radius of this cylinder, and ρ_p, the corresponding electronic density. These two quantities are related such that the averaged density is constant:

$$\pi R_1^2 \left[\bar{\rho} - \rho(\text{cyclo})\right] = \pi R_\text{p}^2 \left[\rho_\text{p} - \rho(\text{cyclo})\right]. \qquad (3)$$

A fit of the experimental results with the condition that, for Φ equal to 1.5%, q^* is equal to the first Bragg peak q_1, gives: $R_\text{p} = 90$ Å. One can then compute the intensity of the first order Bragg peak, $P(q_1)$ divided by the intensity of the second order Bragg peak $P(\sqrt{3}q_1)$. The results are reported in Figure 11 and show a very good agreement with experimental data, once of course the absolute values have been normalised (we arbitrarily chose that for $\Phi = 0.15\%$, experimental and theoretical ratios coincide). For comparison, we also plot the theoretical curve expected in the case of a uniform distribution, which exhibits very small variations around its value for $\Phi = 0\%$.

Thus, we are able to modelize the very strong variation of the intensity of the Bragg peaks with the volume

fraction of particles, by considering a non-uniform distribution of the colloids inside the cylinders with a higher density in the centre: particles are depleted from the walls of the lyotropic cylinders. We find that the depletion thickness is $R_1 - R_p = 60$ Å. The existence of this depletion thickness is the signature of interactions between the solid colloid and the cylinder, the origin of which could be the entropic repulsion due to the surfactant layer coating both the particles and the inner walls of the cylinders. Moreover, this depletion effect explains why particles cannot be incorporated into smaller cylinders.

5 Conclusion

To conclude, we have proven that it was possible to incorporate solid particles into the sufficiently large cylinders of a "swollen" lyotropic hexagonal phase. This new kind of hybrid system, a unidimensional magnetic liquid phase, displays very interesting properties. In this paper, we focus on its structural properties, that we explore by small-angle X-ray scattering. We show that the long-range order of the lyotropic matrix, as well as the initial size distribution of the particles are not perturbed when the particles and the lyotropic system are mixed. The SAXS spectra have illustrated a coupling between particles and lyotropic cylinders; we have shown that it can be modeled by considering that the colloids are depleted from the inner walls of the cylinders.

We have benefited from fruitful discussions with P. Davidson, A-M. Levelut, F. Nallet, V. Ponsinet, M. Veyssié and C. Williams, whom we warmly thank. We also thank V. Cabuil and the Laboratoire de Physico-Chimie Inorganique, Université P. et M. Curie, Paris, for having provided us with the ferrofluid.

References

1. P. Fabre, C. Casagrande, M. Veyssié, V. Cabuil, R. Massart, Phys. Rev. Lett. **64**, 539 (1990).
2. C. Ménager, L. Belloni, V. Cabuil, M. Dubois, T. Gulik-Krzywicki, T. Zemb, Langmuir **12**, 3516 (1996).
3. L. Liébert, A. Martinet, J. Phys. Lett. France **40**, L363 (1979).
4. P. Poulin, V.A. Raghunathan, P. Richetti, D. Roux, J. Phys. II France **4**, 1557 (1994).
5. C. Quilliet, P. Fabre, V. Cabuil, J. Phys. Chem. **97**, 287 (1993).
6. L. Ramos, P. Fabre, E. Dubois, J. Phys. Chem. **100**, 4533 (1996).
7. F. Nallet, D. Roux, C. Quilliet, P. Fabre, S.T. Milner, J. Phys. II France **4**, 1477 (1994).
8. V. Ponsinet, P. Fabre, M. Veyssié, Europhys. Lett. **30**, 277 (1995).
9. L. Ramos, P. Fabre, Langmuir **13**, 682 (1997).
10. T. Dabadie, A. Ayral, C. Guizard, L. Cot, P. Lacan, J. Mater. Chem. **6**, 1789 (1996).
11. R. Massart, IEEE Trans. Magn. **17**, 1247 (1981).
12. J.C. Bacri, R. Perzynski, D. Salin, V. Cabuil, R. Massart, J. Mag. Mag. Mat. **85**, 27 (1990).
13. C. Quilliet, V. Ponsinet, V. Cabuil, J. Phys. Chem. **98**, 3566 (1994).
14. F. Livoland, Y. Bouligand, J. Phys. France **47**, 1813 (1986).
15. V. Ponsinet, P. Fabre, M. Veyssié, L. Auvray, J. Phys. II France **3**, 1021 (1993) .
16. L. Ramos, P. Fabre, L. Fruchter, in preparation.
17. V. Luzzatti, Acta Crystall. **13**, 939 (1960).
18. S. Chandrasekhar, Phil. Trans. Soc. Lond. A **309**, 93 (1983).
19. A. Guinier, *Théorie et technique de la radiocristallographie* (Dunod, Paris, 1956).
20. G. Oster, Riley D. P., Acta Cryst. **5**, 272 (1952).